J. of Wind Engineering
No. 89 October 2001

The Fifth Asia-Pacific Conference on Wind Engineering, Kyoto, 2001 *APCWE V*

A wind tunnel study of separated flow over a two-dimensional ridge and a circular hill

Takeshi ISHIHARA [1], Yozo FUJINO[1] and Kazuki HIBI [2]

1) Department of Civil Engineering, the University of Tokyo, Bunkyo-ku, Tokyo 113-8656, Japan
2) Institute of Technology, Shimizu Corp.,3-4-17, Etchujima, Koto-ku, Tokyo 135-8530, Japan

1. INTRODUCTION

Over the last two decades, turbulent flow over topography has often been studied, because of its importance in a wide range of subjects, such as the safety of structures, extraction of wind energy, pollutant dispersion, wind damage to agriculture and forestry, and aviation safety. Reviews of recent developments which focus on neutrally stratified turbulent flow over topography were covered by Taylor, Mason & Bradley [1] and Finnigan [2]. These reviews provide some understanding of how a specified upwind mean flow and turbulence should be modified on passing over low hills with a moderate slope. Detailed information on separated flow over a two-dimensional ridge and a circular hill is lacking, although some wind tunnel studies have been conducted for a two dimensional ridge (see, Arya et al. [3], Ruck & Adams [4], Almeida et al. [5]), and for a three dimensional hill (see, Castro & Snyder [6], Arya & Gadiyaram [7], Utnes & Eidsvik [8], Ishihara et al. [9]).

In the current study, we applied split-fiber probes to measure three velocity components in order to provide details of mean velocity and turbulence statistics of separated flow over a two-dimensional ridge and a circular hill, and shed some light on the structure of the turbulent flow in the near-wake region. The experimental emphases are on the three-dimensionality of the separated flow and surface roughness effect.

2. EXPERIMENTAL DETAILS

2.1 Facility

The present study was conducted in a return wind tunnel, which has a working section of 1.1 m wide, 0.9 m high and 7 m long. A neutrally stratified atmospheric boundary layer was simulated, using two 60 mm high cubic arrays placed just downstream of the contraction exit and followed by 20 mm and 10 mm cubic roughness element, covering 1.2 m of the test-section floor. The remaining 5.8 m of the test-section floor was covered with plywood for the smooth case and with an artificial grass 5mm high (z_r) for the rough case. The wind speed outside the boundary layer U_{ref} was monitored throughout the experiment using a Pitot tube and maintained at 5.8 m/s. The resulting boundary layer was about 0.36 m thick (δ) at the point where the hill was mounted and the scale of the simulated boundary layer was about 1/1000 of the atmospheric boundary layer, on the basis of the power spectra of the longitudinal velocity component.

The model hill was machined from wood and had a cross-section of $z_s(r)=H\cos^2(\pi r/2L)$ with H =40 mm and L =100 mm. The maximum slope was thus about 32°. Fig. 1 shows details of the hill and coordinate system used in the study, where x, y and z are the streamwise, spanwise and vertical directions, respectively. In the x-coordinate, zero is the center of hill (4.6 m downstream of the contraction exit). A second vertical coordinate, $z'=z-z_s(r)$, is also used to denote height above the local surface.

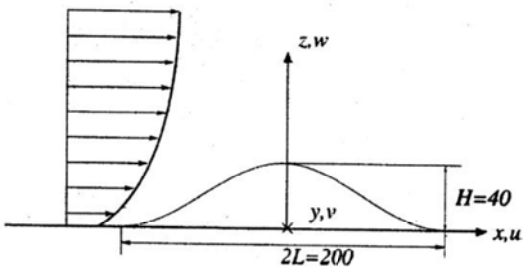

Fig. 1 Notations used in this study.

Four hill models were examined: two ridges and two circular hills. The two ridges have different surface roughness. For the rough case, the ridge surface was covered with the same artificial grass as used for the surrounding surface, and for smooth

case no any roughness element was used. They are henceforth labelled as 2dr and 2ds. The ridge spanned the entire tunnel width. The two corresponding circular hills were also covered with and without the grass, and are marked as 3dr and 3ds. For each case, the roughness of the hill surface was identical to that of the surrounding terrain.

The main aerodynamic parameters in the experiment are summarized in Table 1, where the dimensionless parameters, $R_{eH}(=U_H H/\nu)$ and $R_*(=u_* z_0/\nu)$, denote the global and surface Reynolds number, respectively. For the smooth case, R_* was less than the critical value of 2.3. This implies that the flows over the smooth ridge and hill were not quite fully aerodynamically rough and were slightly dependent on the Reynolds number. For the rough case, R_* was larger than the critical value, indicating that there were no Reynolds effect in these cases.

Table 1 Main aerodynamic parameters in the experiment

Case	δ/H	z_r/H	H/z_0	Re_H	R_*
2ds	9.0	0	4000	1.2×10^4	0.14
2dr	9.0	0.125	133	1.0×10^4	6.4
3ds	9.0	0	4000	1.2×10^4	0.14
3dr	9.0	0.125	133	1.0×10^4	6.4

2.2 Velocity measurements

Velocity measurements in the undisturbed boundary layer were made using constant temperature hot-wire anemometers (DANTEC 56C01 and 56C17) with cross-wire probes (55R53 and 55R54). The X-wires were calibrated against a Pitot tube in the free stream. The drifts in calibration coefficients were very small, since temperature in the tunnel was fixed during data acquisition. Since X-wire probe anemometers for turbulence measurement cannot give reasonable accuracy when the turbulence intensity are larger than 0.3, all velocity measurements around the hill were made with two kinds of split-fiber probes. The detailed information on the probes and the calibration procedures have been described in detail by Ishihara et al. [9].

3. RESULTS AND DISCUSSION

3.1 Flow characteristics in the undisturbed boundary layer

Fig. 2 shows the profiles of mean velocity U and turbulence intensity I_u in the undisturbed boundary layer. The velocity profiles are adequately represented by a logarithmic law, $U/u_*=\kappa^{-1}/\ln(z/z_0)$, in the surface layer. Considering that the simulated boundary layer has a scale of 1/1000, the equivalent full scale z_0 is 0.01 m, which is characteristic of a grass or heather covered hill and 0.3m is that of a forest covered hill.

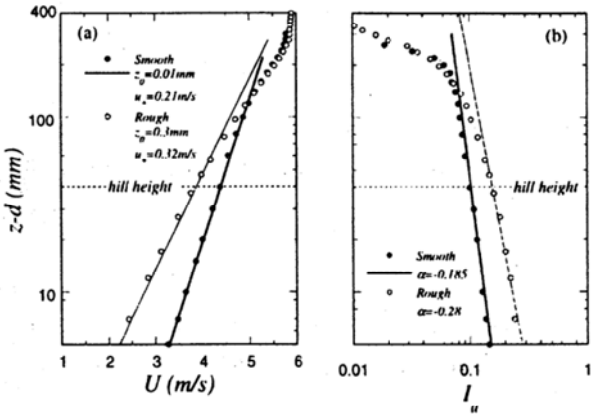

Fig. 2 Vertical profiles of mean velocity and turbulence intensity over the flat floor.

3.2 Mean flow field

Three velocity components were measured in the symmetric plane (y/H=0) for all configurations. Fig. 3 shows vertical profiles of mean velocity components of U for each case. The profile in the undisturbed (no-hill) boundary layer (dashed line) is superimposed on the local profiles. The mean velocity components are normalized by the free-stream velocity U_{ref}. The dashed-dot line in the figures is the locus of zero streamwise velocity. It can be seen that streamwise mean velocity U are the increase in velocity near the surface on the hilltop, the slight deceleration at the upwind hill foot, and the flow separation behind the hill.

Some features are worthy of particular comment. First, a strong shear layer forms immediately downstream of the top of the hill. This layer is identified by a point of inflection in $U(z)$, high values of the mean shear $\partial U/\partial z$, and also by high values of the Reynolds stress (see later).

The second notable feature of Fig. 3 is that the reversed flow region behind the two smooth cases (2ds and 3ds) is much smaller than those behind the corresponding rough cases (2dr and 3dr). The present result implies an exactly opposite trend to the classic case of surface-roughened cylinders or spheres in free flow, where the added roughness causes laminar-turbulence transition and delays flow separation, resulting in a small recirculation. On the other hand, within turbulent boundary layers, added roughness decreases mean velocity in the surface layer (see, Fig.2) and leads to an earlier flow separation, resulting in a large recirculation.

The third feature is that the downstream extents of the recirculating region of the two-dimensional ridges are longer than those of the three-dimensional hills. Separation bubble sizes obtained in the present study are summarized in Table 2.

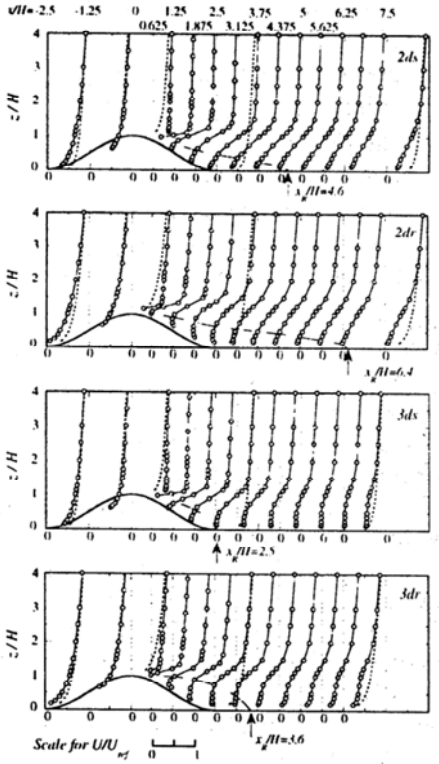

Fig. 3 Vertical profiles of the streamwise velocity components normalized by the reference velocity.

Table 2 Separation bubble size (distances are relative to hilltop)

Case	Separation X_s/H	Reattachment X_r/H
2ds	1.1	4.6
2dr	0.6	6.4
3ds	0.9	2.5
3dr	0.6	3.6

Fig. 4 illustrates the mean velocity vectors and the streamlines in the symmetric plane over the smooth ridge (2ds) and the smooth hill (3ds). The flow patterns for both cases are quite similar on the upwind side, but are considerably different on the lee side. The most striking behaviour is that opened streamlines are shown in the three-dimensional wake, while closed ones are revealed in the two-dimensional case. The reason why the flow pattern changes can be interpreted using the continuity equation. In the case of two-dimensional separation, the circulating flow must be formed to satisfy the continuity equation. While in the case of three-dimensional separation it is possible to satisfy the continuity equation without the circulating flow, since the spanwise flow exists. Namely, when flow field in the central plane is considered as a two-dimensional field, the term of $\partial v/\partial y$ becomes a source as $\partial v/\partial y$ is negative or a sink as $\partial v/\partial y$ is positive in the fictitious two-dimensional field, as pointed out by Ishihara and Hibi [10]. Fig. 5 shows a schematic diagram of flow field around a circular hill.

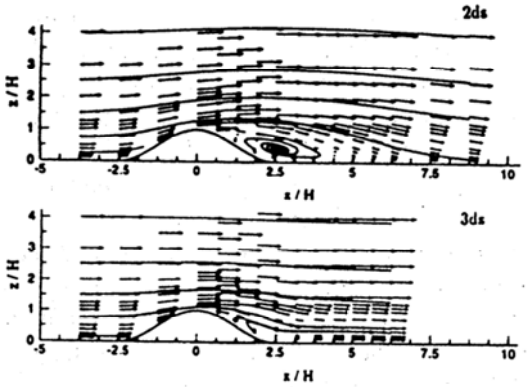

Fig. 4 Mean velocity U, W vectors in the y=0 plane.

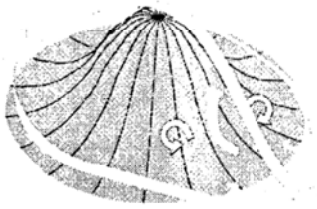

Fig. 5 Schematic diagram of flow field around a circular hill.

3.3 Reynolds stress field

Besides the mean velocity, it is of interest to know how turbulence might be modified as the flow goes over the hill.

Figs. 6, 7, 8 show vertical profiles of three normal stress components, σ_u, σ_v and σ_w in the symmetric plane for each case. The profile in the undisturbed (no-hill) boundary layer (dashed line) is also superimposed on the local profiles. The solid lines in these figures are the locus of maximum values.

Relative to upwind, σ_v displays some increase at low levels from the upwind deceleration region to the hilltop, while the increase in σ_u as well as that in σ_w are very slight. On the other hand, on the lee slope, all three normal stress components show strong peaks around the regions of maximum shear in the streamwise velocity profiles. It is clear that these highly turbulent energies are generated by the flow separated on the lee slope of the ridges and hills and far in excess of those that occur in the undisturbed boundary layer. In the recirculation zone, all normal stress components are below their upwind values, with greater reductions associated with the increasing surface roughness.

In the near-wake region beyond the separation bubble, the profiles of σ_u and σ_w are substantially rounded and the peak values decay with the downstream distance. The most striking behaviour in the three-dimensional wake is that σ_v profiles show second local maxima in the so-called wall layer,

which could not be observed in the two-dimensional wake. In this layer, the σ_u profiles show a roughly constant value. These second maxima in the σ_v profiles are conjectured to be generated by a low frequency motion as pointed out by Ishihara et al. [9]. It should be noted that for the rough hill the second peaks in the σ_v profiles are weak, indicating that increase of surface roughness will reduce turbulent motion in the spanwise direction. Table 3 shows maximum values of the ratio of normal stresses over the topography to those in the undisturbed boundary. It can be seen that the three normal stresses of the smooth hill gives the largest values.

Table 3 The ratio of normal Reynolds stresses to those in the undisturbed boundary layer.

Case	$(\sigma_u/\sigma_{u0})_{max}$	$(\sigma_v/\sigma_{v0})_{max}$	$(\sigma_w/\sigma_{w0})_{max}$
2ds	2.9	2.7	4.3
2dr	1.8	1.9	2.4
3ds	3.0	3.4	4.6
3dr	1.9	1.7	2.1

4. CONCLUSION

A wind tunnel experiment of separated flows over a two-dimensional ridge and a circular hill have been performed. Mean flow and turbulence were measured using split-fiber probes designed for measuring flows with a high turbulence and separation. Principle results are:

1) The cavity zones behind circular hills are smaller than those behind two-dimensional ridges, because of the convergence of flow in the three-dimensional wake.
2) The increased roughness on the hill surface causes an earlier separation, resulting in a large recirculation zone.
3) The lateral velocity variances behind the circular hills show second local maxima in the wall layer, which are generated by a crosswind motion and cannot be observed in the two-dimensional cases.

References

1) P.A. Taylor, P.J. Mason and E. F. Bradley, Boundary-Layer Meteo., Vol. 39, 1987, pp.107-132.
2) J.J. Finnigan, Flow and Transport in the Natural Environment (ed. W. L. Steffen and O. T. Denmead), Springer, 1988, pp.183-229. .
3) S. P. S. Arya, M. E. Capuano and L. C. Fagen, Atmos. Environ. Vol.20, 1987, pp.753-764.
4) B. Ruck and E. Adams, Boundary-Layer Meteo.,Vol.56, 1991, pp.163-195.
5) G. P. Almeida, D. F. G. Durao and M. V. Heitor, Experimental Thermal and Fluid Science, Vol.7, 1993, pp.87-101.
6) Castro I.P. and Snyder W.H., Atmos. Environ. 16, 1982, pp.1869-1887.
7) Arya S.P.S. and Gadiyaram P.S., Atmos. Environ. 20, 1986, pp.729-740.
8) T. Utnes and K. J. Eidsvik, Boundary-Layer Meteo., Vol.79, 1996, pp.393-416.
9) T. Ishihara, K. Hibi and S. Oikawa, J. Wind Eng and Ind. Aero., Vol. 83, 1999, pp. 95-107.
10) T. Ishihara and K. Hibi, Proc. of the 3rd. International Symp. on Comp. Wind Eng., 2000, pp. 99-102,.

Key words: tow-dimensional ridge, circular hill, separation, Roughness effects, turbulence

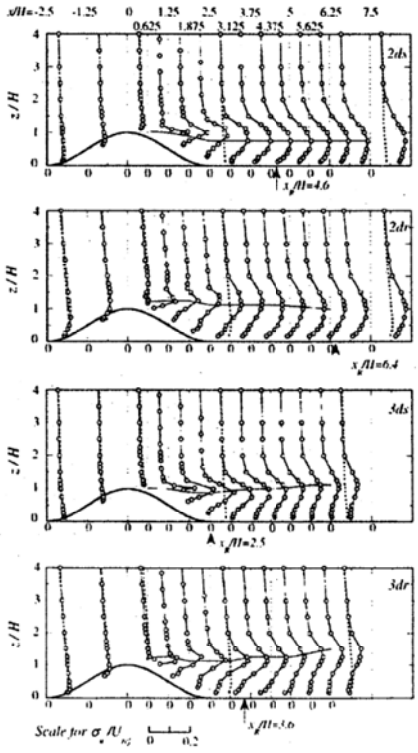

Fig. 6 Vertical profiles of σ_u.

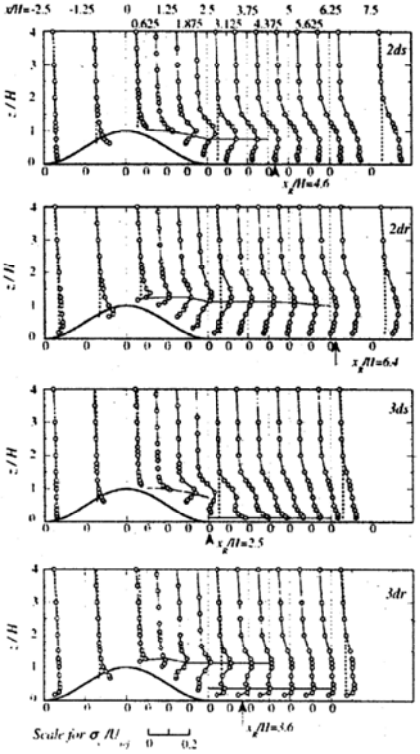

Fig. 7 Vertical profiles of σ_v.

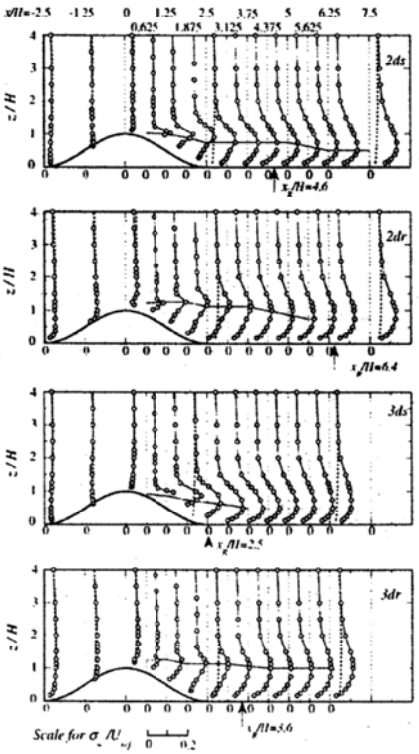

Fig. 8 Vertical profiles of σ_w.